J Mater Sci (2012) 47:6346–6353
DOI 10.1007/s10853-012-6559-z

Al_2O_3 particle rounding in molten copper and Cu8wt%Al

C. Krüger · A. Mortensen

Received: 2 February 2012 / Accepted: 5 May 2012 / Published online: 26 May 2012

Abstract We investigate processing-microstructure relationships in the production of Al_2O_3 particle reinforced copper composites by solidification processing. We show that during production of the composites by gas-pressure infiltration of packed Al_2O_3 particle preforms with liquid Cu or with liquid Cu8wt%Al at either 1,150 or 1,300 °C, capillarity-driven transport of alumina can cause rounding of the Al_2O_3 particles. We use quantitative metallography to show that the extent of particle rounding increases markedly with temperature and with the initial aluminum concentration in the melt. An analysis of the thermodynamics and kinetics governing the transport of alumina in contact with molten copper, considering both interfacial and volume diffusion, leads to propose two mechanisms for the rounding effect, namely (i) variations in the equilibrium concentration of oxygen in the melt as affected by the initial aluminum concentration, or (ii) segregation of aluminum to the interface with the ceramic.

Introduction

Copper and alumina do not have much affinity for one another: the wetting angle of liquid Cu on Al_2O_3 is high (128° [1]) and the intrinsic strength of the interface between the two is low [2–5]. Yet, combining the two phases in a composite material has clear technological potential [6–9]: copper is an excellent heat and electricity conductor, in which Al_2O_3 particles offer improved hardness and wear resistance without introducing atom-scale electron scattering centers. The Cu–Al_2O_3 system is non-reactive in high-vacuum or in oxygen-lean inert gas [4]; as a consequence Al_2O_3 should not be degraded during processing. It is also documented that Al_2O_3 in liquid Cu shows minimal grain boundary grooving [10] and that triple lines in sessile drop experiments show minimal ridging (on the order of 40 nm) [10, 11]. One therefore would expect Al_2O_3 reinforcements to be geometrically stable in molten copper. We show here that this is not always so: if aluminum is present in the copper matrix, significant capillarity-driven motion of the matrix/alumina interface may occur if the composite is exposed to elevated temperature. This has implications for the processing of copper-matrix composites, and also for other processes such as the brazing of alumina with copper-based alloys.

C. Krüger (✉) · A. Mortensen
Laboratory for Mechanical Metallurgy, Institute of Materials,
École Polytechnique Fédérale de Lausanne, Station 12,
CH-1015 Lausanne, Switzerland
e-mail: krueger_carmen@web.de

Experimental procedure

Production of the composites

Metal matrix composites of this work were produced by pressure-driven infiltration of ceramic powder preforms with liquid metal [12] using the following procedure. Cu and Cu8wt%Al (Cu8Al) ingots are alloyed and cast from pure Al and Cu (both 4 N) in graphite crucibles using a high-vacuum induction furnace under static argon. The particles used to produce the composites are α-Al_2O_3 F1000 purchased from Treibacher Schleifmittel (Laufenburg, Germany), of 99.5 % purity (the main impurity present being Na). The mean particle diameter D(v, 0.5), measured by laser diffraction in a Mastersizer (Malvern, UK), is 4.4 μm. The particles are of angular form (having visibly been produced by comminution). Preforms are

prepared by packing the powder directly into Al_2O_3-crucibles, using both tapping and mechanical vibration. The metal ingot (diameter 15 mm, length 40 mm) is placed on top of the preform in the crucible which is then placed within a pressure-infiltration apparatus (described in [13]). Induction heating is started once a stable primary vacuum is reached. Infiltration is then conducted at a pressure of 8 MPa applied for three minutes at temperatures of 1,150 or 1,300 °C, this fills all pores within the preform. After infiltration, the composite is cooled within the apparatus by switching off the induction furnace while maintaining the applied pressure and the flowing water cooling system. For all data presented in what follows, infiltration was done simultaneously with Cu and Cu8Al in one experiment with two crucibles to insure that both specimens undergo exactly the same time-temperature cycle. Composites are named according to the matrix and their infiltration temperature: Cu-1150 for example designates a composite infiltrated with pure copper at 1,150 °C.

Characterization

For microstructural characterization sample sections were polished and observed in a scanning electron microscope (SEM), equipped with energy-dispersive X-ray spectroscopy (Fei, Hillsboro, US). Quantitative image analysis was conducted to extract two geometrical characteristics of the particle/matrix interface. The first is the circularity of individual Al_2O_3 particles in each composite, C, defined as

$$C = 4\pi \frac{A}{P^2} \quad (1)$$

where A is the measured area of the particle and P its perimeter along a metallographic cut. By applying this equation one compares the area of the particle with that of a circle having the same perimeter [14]. C was measured using the "image j" software [14] on five backscattered electron images having the same magnification for each composite, taken at random locations along a single polished surface. A second, more local, measure of curvature along the metal/ceramic interface was collected by computing the (two-dimensional, 2D) curvature at various points along its intersection with the metallographic planes of polish. The local curvature at points along the interface of randomly chosen particles was determined using the National Instruments "Vision Assistant 2011" software and its "Contour Analysis" function. More specifically, the interfacial line, separating dark (alumina) and bright (metal) phases, is identified by thresholding, parameters of which are defined by the user so as to obtain a clear and realistic contrast between alumina particles and copper matrix. Once the interfacial line is found, the software calculates curvature values by fitting a cubic b-spline function to three equidistant points along the interface line, as documented in [15]. Parameters were kept constant for all images and all samples analyzed. For each composite we measured 6,000 curvature values, excluding broken particles or contact points between particles. The particle morphology was also investigated by SEM after dissolution of the metallic matrix with nitric acid (38 %). The remaining powders were inspected by X-ray diffraction on a D8 Bruker diffractometer (Karlsruhe, Germany) equipped with a Cu K_α radiation source.

Results

Microstructure of the composites

The microstructures of infiltrated composites consist of homogeneously distributed ceramic particles in a pore-free metallic matrix. In all three of Cu-1150, see Fig. 1a, Cu-1300, see Fig. 1b and Cu8Al-1150, Fig. 1c, the Al_2O_3 particles show little, if any, change in morphology. On the other hand, Cu8Al-1300 composites show visible rounding of the Al_2O_3 particles (Fig. 1d).

Diffraction data

Diffractograms taken of infiltrated Al_2O_3 powders that were removed from infiltrated composites after matrix dissolution show no change compared with diffractograms of the initial Al_2O_3-F1000 powder (Fig. 2). In both, the presence of some $NaO_2 \cdot 11Al_2O_3$ is noted. This phase is also called β-Al_2O_3; it is stabilized by the presence of NaO_2 initially present within the alumina powder. There is no sign of ternary oxides such as $CuAlO_2$ or $CuAl_2O_4$, which is not surprising since, at the low oxygen partial pressures in the infiltration apparatus [16], these are not thermodynamically stable [17].

Particle morphology

Measured values of the shape descriptor C are in Table 1. Circularity is clearly raised and highest after infiltration with Cu8Al at 1,300 °C. Cu-1300 and Cu8Al-1150 composites show a slightly higher circularity that does Cu-1150; however, the difference is small and might be within experimental uncertainty. Simple visual examination of polished composite cross-sections confirms significant particle rounding in Cu8Al-1300. It is on the other hand harder to conclude that particle rounding occurred in Cu-1300, Cu8Al-1150 or Cu-1150. Comparing SEM images of Al_2O_3-particles removed from the composites by copper dissolution, one finds no difference in angularity between the initial Al_2O_3-powder, see Fig. 3a, and powder infiltrated with Cu at 1,150 °C, see Fig. 3c.

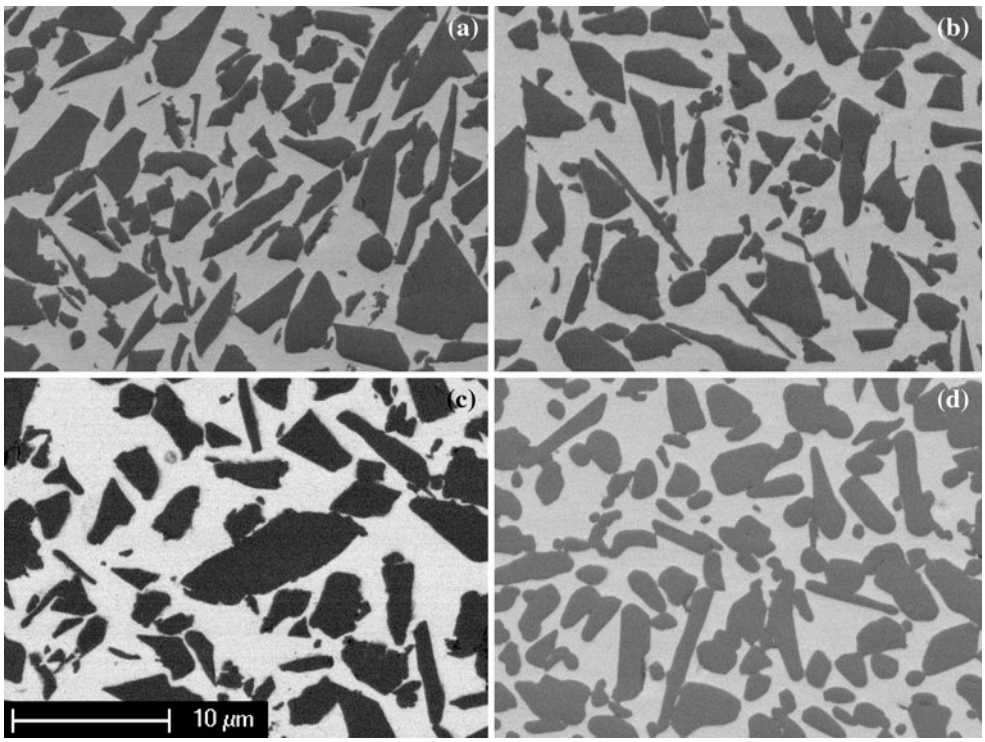

Fig. 1 Al_2O_3 infiltrated with **a** Cu at 1,150 °C, **b** Cu at 1,300 °C, **c** Cu8Al at 1,150 °C, **d** Cu8Al at 1,300 °C

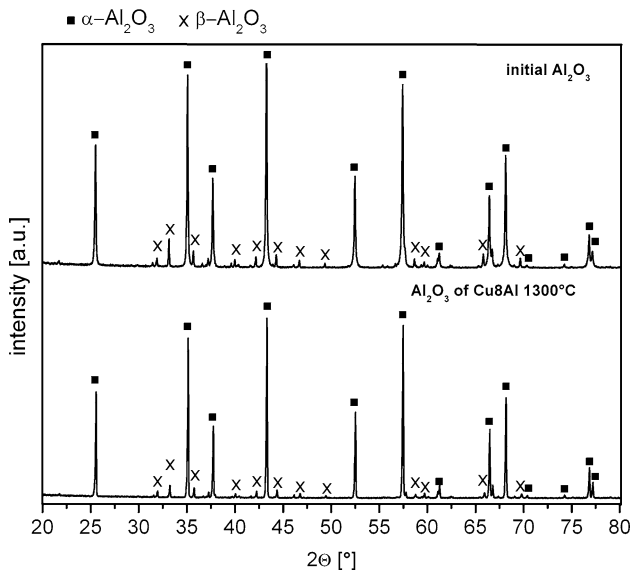

Fig. 2 Diffractogram of initial Al_2O_3 powder (*top*) and Al_2O_3 powder infiltrated with Cu8Al at 1,300 °C (*bottom*)

Table 1 Minimal and maximal circularity obtained by image analysis

Matrix-T_{inf}	Cu-1150 °C	Cu-1300 °C	Cu8Al-1150 °C	Cu8Al-1300 °C
C	0.59–0.64	0.65–0.68	0.65–0.66	0.70–0.72

All data thus indicate that no discernible rounding occurs during infiltration with pure copper at 1,150 °C. On the other hand, Al_2O_3 infiltrated with Cu8Al at 1,300 °C again shows clearly rounded particles, see Fig. 3f, in agreement with Fig. 1d and quantitative circularity analysis (Table 1). The powders from composites Cu-1300, Fig. 3d and Cu8Al-1150, Fig. 3e, seem to have somewhat less sharp edges than do Al_2O_3 particles removed from Cu-1150. This would agree with the circularity values, but again the difference is slight and therefore inconclusive. To evidence any role of solid-state sintering of the Al_2O_3-particles during heat-up, we also heated a preform under the same conditions as used for infiltration at 1,300 °C, and then cooled the preform without metal infiltration. The heated powders can be seen in Fig. 3b: dry heat-up causes no particle rounding. Rounding of the Al_2O_3-particles thus occurs only if the particles are in contact with the liquid metal.

To quantify the extent of particle rounding, we also measured the local curvature distribution along the particle/matrix interface of 2D metallographic sections, as described above. These measurements have the following simple significance: if transport smoothens the particles to eliminate any (true 3D) curvature exceeding a certain value, the 2D curvature distribution measured on random metallographic cuts through the composite will also be eliminated above a certain value (which must be on the order of one-half the peak 3D curvature). The data are summarized in

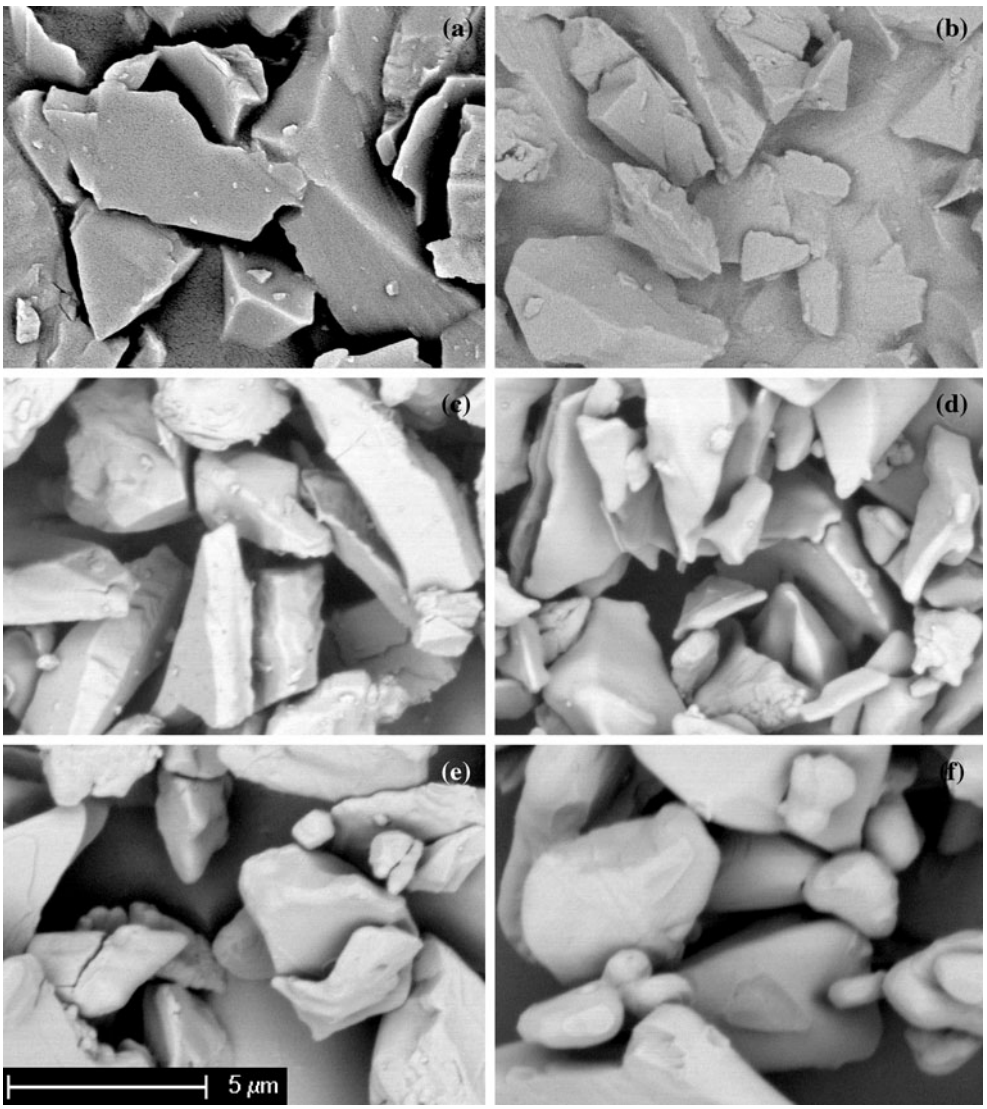

Fig. 3 Al_2O_3 particles: **a** initial powder, **b** after heating to 1,300 °C and from infiltrated composites after dissolution of the matrix: **c** Cu-1150, **d** Cu-1300, **e** Cu8Al-1150, **f** Cu8Al-1300

cumulative curvature probability plots. These give the probability that the measured local matrix/particle 2D interface curvature exceed a certain value versus the local 2D curvature, see Fig. 4. The right-hand portion of the plot is shaded in gray, to indicate that data in that area have little real value since above a curvature of 10 μm^{-1}, corresponding to a radius of curvature of 100 nm roughly four pixels long, the resolution limit of the calculation method has been met.

As a reference for low-temperature infiltration, we have added to Fig. 4 data gathered similarly from a composite of the same F1000 Al_2O_3 powder infiltrated with Al2wt%Cu at 750 °C, (micrographs of this composite are given in [18]). We note in passing that its matrix being softer, it polishes with more difficulty than copper-matrix composites and hence a smaller proportion of the particle/matrix interface was amenable to analysis. From this graph, it is evident that the particles infiltrated at 1,300 °C with Cu8Al show a much lower probability for having highly curved metal/ceramic interfaces. The cut-off of this curve (corresponding to the highest expected interface curvature value in the composite) is far lower that it is with the four other composites. This can be located at a curvature of 3.5 μm^{-1} which corresponds to a radius of curvature of 285 nm. All other curves are similar: no difference was thus found between the remaining composites: F1000 alumina infiltrated with Cu at 1,300 °C, Cu or Cu8Al at 1,150 °C and the same powder infiltrated with Al2wt%Cu near 700 °C, all of which have interfaces curved down to a radius of 100 nm or lower.

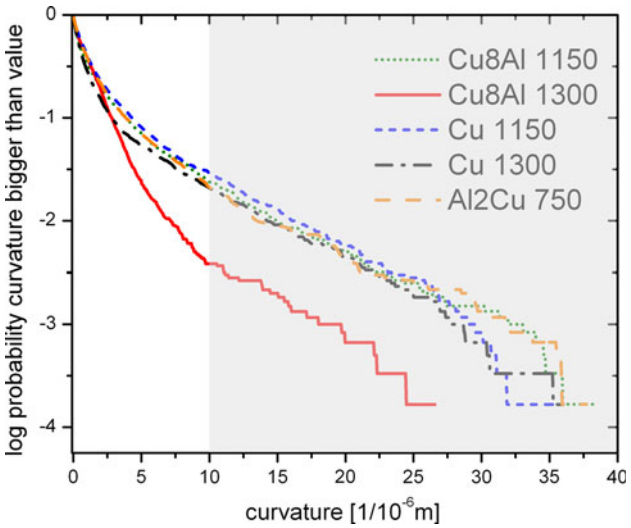

Fig. 4 Cumulative probability plot of interfacial curvature along metallographic cuts of infiltrated Al_2O_3 particulate composites showing a cut-off curvature around 3.5 μm^{-1} for Cu8Al-1300 (*shaded area* represents measurements deemed imprecise; see main text)

Discussion

Kinetics of particle rounding

In summary, curvature reductions observed in the present composites are small: there is no extensive coarsening or sintering of the ceramic particles, be it before infiltration or in the composite, even after exposure to 1,300 °C. Still, exposure of the alumina particles to molten Cu8Al at 1,300 °C is shown to reduce interfacial curvature gradients, resulting in the rounding of sharp corners and smoothening of protrusions or crevices that might have initially been present along the particle surface. The effect is visible in the composite microstructure and also on leached particles, and is also evidenced quantitatively by measuring the circularity of the particle perimeters or the distribution of interfacial curvature on metallographic cross-sections of the composite. Such reductions in interface curvature are driven by capillary forces and necessitate transport of the alumina within the composite. Excluding diffusion through the refractory alumina phase (the diffusion coefficient of oxygen through bulk alumina is on the order of 10^{-23} m^2/s at 1,300 °C [19]) transport occurs either along the metal/ceramic interface, or through the liquid copper matrix.

Simple geometrical versions of this capillarity-driven transport process are the rounding of a harmonically perturbed spherical particle or the decay of a sinusoidal perturbation along a flat interface between alumina and the matrix. We use these as a yardstick to quantify the kinetics of particle rounding in the present composites: we take it that the metal/ceramic interface will not be more curved than harmonic perturbations to a sphere or sinusoidal perturbations of a flat interface that have had time to decay after exposure to a thermal cycle identical to those seen by the composite during infiltration. Nichols and Mullins [20] give explicit expressions for the rate of decay of such perturbations by either surface or volume diffusion (see Table 1 of that reference). From these, one can calculate the time Δt, that is needed to reduce the amplitude of a perturbation to 1 % of its initial value, by volume diffusion through the liquid metal or by interface diffusion. For volume diffusion

$$\Delta t = \frac{R_0^3 kT}{D_V c_O \gamma \Omega^2} \cdot \frac{1}{\alpha_V} \tag{2}$$

where k is the Boltzmann constant, T the absolute temperature, D_V the volumetric diffusion coefficient, c_O the concentration of the diffusing species in the melt in numbers of atoms per m^3, and γ the interfacial energy (assumed isotropic); for pure Cu on Al_2O_3 we take $\gamma = 1.91$ J/m^2 using Young's equation and data from [4]. Ω is the volume of alumina per atom of the rate-controlling diffusing species (O or Al) and α_V is a constant. For spheroidization of a harmonically perturbed sphere, R_0 is the particle radius and α_V depends on l, the degree of the spherical harmonic perturbation: α_V increases with l and equals roughly 3 for $l = 2$. For sinusoidal perturbations of a flat interface, if R_0 is the perturbation half-wavelength, $\alpha_V \approx 7$. For interfacial diffusion, one has

$$\Delta t = \frac{R_0^4 kT}{w D_I \gamma \Omega} \cdot \frac{1}{\alpha_I} \tag{3}$$

where D_I is the diffusion coefficient for interface diffusion, w the width of the layer in which interfacial diffusion occurs (note that only the product of both, i.e., the interfacial diffusivity wD_I is directly measurable). $\alpha_I \approx 5$ for $l = 2$, increasing again with l, while for sinusoidal perturbations along a flat interface $\alpha_I \approx 21$.

To calculate c_O in the melt, one needs to account for the dissolution of Al_2O_3 in liquid Cu, given by:

$$\langle Al_2O_3 \rangle \rightleftharpoons 2(Al)_{(Cu)} + 3O_{(Cu)} \tag{4}$$

$$RT \ln K_r = \Delta G^f_{Al_2O_3} \tag{5}$$

where R is the ideal gas constant, K_r the equilibrium constant and $\Delta G^f_{Al_2O_3}$ the Gibbs energy for formation of Al_2O_3 from pure liquid Al and pure O_2 at a pressure of one atmosphere. At 1,423 K $\Delta G^f_{Al_2O_3} = -1,224$ kJ/mol; this becomes −1,176 kJ/mol at 1,573 K [21]. The equilibrium constant K_r is expressed as a function of the different activities a_i:

$$K_r = a^2_{Al_{(Cu)}} a^3_{O_{(Cu)}} \tag{6}$$

The activities a_i are the product of the mole fraction x_i by the activity coefficient γ_i:

$$a_i = \gamma_i x_i \tag{7}$$

The reference states are pure liquid Al and pure O_2 at a pressure of one atmosphere, respectively. $\gamma_{Al} = 0.002$ in pure copper [22] at 1,373 K, and for simplicity (given other, greater, sources of uncertainty) we take γ_{Al} to be constant at 0.002: its variation with temperature between 1,373 and 1,473 K is only from 0.003 to 0.001 [23]. $\gamma_O = 0.18$ at 1,423 K and 0.32 at 1,573 K [24]. If superscript 0 indicates the initial species concentration before dissolution, then:

$$(x_{Al} - x^0_{Al}) = \frac{2}{3}(x_O - x^0_O) \tag{8}$$

due to stoichiometry of dissolution. We thus have:

$$\left(\frac{2}{3}x_{O_{(Cu)}} - \frac{2}{3}x^0_O + x^0_{Al}\right)^2 x^3_{O_{(Cu)}} = \frac{\exp\left(\Delta G^f_{Al_2O_3}/RT\right)}{\gamma^2_{Al}\gamma^3_O} \tag{9}$$

which allows us to estimate the oxygen and aluminum concentrations in the liquid metal at different infiltration temperatures. If the initial concentration of aluminum and oxygen is ≈ 0, then $x_{Al} = \frac{2}{3}x_O$ and we obtain $x_O = 4 \times 10^{-8}$ at 1,423 K and 4.4×10^{-7} at 1,573 K. It is worth noting that the oxygen partial pressure in the pressure-infiltration apparatus being below 5×10^{-23} atm at 1,200 °C [16], the atmosphere in contact with the melt does not increase x_O above the value dictated by alumina dissolution. However, we cannot exclude that oxygen initially present in the solid copper ingot remains in the copper melt, although the melt is in contact with an atmosphere poor in oxygen. If we estimate an upper bound of remaining oxygen in the melt from its purity, then we take $x^0_O = 10^{-4}$ (corresponding to 100 ppm) and $x^0_O = 10^{-5}$ (corresponding to 10 ppm) and calculate the aluminum concentration according to Eqs. (8) and (9). The concentrations are then very low; $x_{Al} = 2 \times 10^{-13}$ at 1,423 K and 8×10^{-11} at 1,573 K for $x^0_O = 10^{-4}$ and $x_{Al} = 7 \times 10^{-12}$ at 1,423 K and 3×10^{-9} at 1,573 K for $x^0_O = 10^{-5}$. The Al and O concentrations being potentially very different, and the re-deposition of both Al and O atoms being needed for the rounding of Al_2O_3, it is the rate of diffusion of the species having the lower concentration that is rate-limiting. We therefore take c_O to be the concentration of the minority species (aluminum if $x^0_O = 10^{-4}$ or 10^{-5}).

The Cu–Al_2O_3 system

With the above assumptions and $\Delta t = 180$ s (the time during which the infiltration temperature was maintained in experiments) Eqs. (2) and (3) give estimates of R_0, the smallest radius of curvature one expects to observe along the metal/ceramic interface after infiltration. In pure copper no particle rounding occurs, so that R_0 must be smaller than 100 nm at both temperatures. In turn this implies (Eqs. 2, 3) that D_V be of order 10^{-8} and 10^{-9} m^2/s or smaller at 1,423 and 1,573 K, respectively, if the initial melt is oxygen-free. In terms of volume diffusivity $x_i D_V$ this implies values of 1.1×10^{-15} m^2/s at 1,423 K and 1.2×10^{-15} m^2/s at 1,573 K; this is of the same order of magnitude as the value given in [10], namely 7.8×10^{-16} at 1,423 K. In general, values for D_V in liquid metals are on the order of 10^{-8}–10^{-9} m^2/s [25]; for pure liquid copper the coefficient for self-diffusion in the temperature range 1,400–1,600 K is roughly 5×10^{-9} m^2/s [26]. Also, the diffusion coefficient for oxygen in liquid copper is 1×10^{-8} and 1.2×10^{-8} m^2/s at 1,423 and 1,573 K, respectively [27]. The lack of measurable rounding at both temperatures is thus a priori surprising; however, we note that volume diffusion of Al_2O_3 in the liquid Cu melt is likely not to be a process of parallel independent diffusion of oxygen or aluminum atoms. The reason is that oxygen and aluminum atoms interact strongly and therefore probably form clusters in the liquid [2, 4]. Diffusion coefficients for clusters of Al and O in liquid Cu have not been measured to our knowledge, but it is likely that Al–O clusters would diffuse much slower than isolated oxygen or aluminum atoms in liquid Cu, explaining that their mobility be reduced below 10^{-9} m^2/s.

If on the other hand oxygen is initially present in the melt at concentrations of $x^0_O = 10^{-4}$ or $x^0_O = 10^{-5}$, the aluminum concentrations become too low to allow any morphology changes: a D_V of 2×10^{-5} or of 5×10^{-7} m^2/s, respectively, would be required to explain rounding of up to 100 nm. In both cases, namely $x^0_O = 100$ and 10 ppm, the low aluminum concentrations give the volume diffusivity $x_{Al}D_V$ such low values that coarsening is essentially non-operative. We view this scenario as possible, but not likely given that micrographs betray, as mentioned earlier, a slight visual difference between the initial particle roughness, see Fig. 3a–c and that of particles dissolved from composite Cu-1300, see Fig. 3d.

According to the same argumentation as for D_V, $D_I\omega$ must be lower than a value near 10^{-22} m^3/s at both 1,423 and 1,573 K. $D_I\omega$ was estimated in [10] from grain boundary grooving experiments at 1,423 K as $D_I\omega = 3 \times 10^{-22}$ m^3/s. The activation energy for interface diffusion in the Cu–Al_2O_3 system is to our knowledge not known; we thus use values of the activation energy for surface diffusion along solid Al_2O_3, which can be found in [28]. Taking a median value of values quoted, namely $Q = 400$ kJ/mol, to estimate wD_I at temperatures other than 1,423 K, we obtain 1×10^{-20} m^3/s at 1,573 K. This value is higher than the interfacial diffusivity upper bound suggested by our experiments.

The Cu8Al–Al_2O_3 system

To conduct the same calculations for Al_2O_3 in a Cu8Al melt, one needs to estimate the oxygen concentration in the melt. To this end, one has to take into account the strong interactions between Al, now at a high concentration ($x_{Al} \geq 0.17$), and dissolved O in the liquid, as the significant amount of aluminum present is likely to cause γ_O to deviate from unity. This may be described using Wagner's first-order interaction parameter ε_O^{Al} defined by $\ln\gamma_O = \varepsilon_O^{Al} x_{Al}$; however, no value was found in the literature. An estimation according to the quasi-chemical method of Jacob and Alcock [29] also could not be made, as we know of no value for the activity coefficient of oxygen in liquid Al at infinite dilution. ε_O^{Al} must, however, be strongly negative, as Al and O interactions are known to be very strong. The presence of a significant quantity of aluminum in the melt should therefore a priori cause a strong decrease in the activity coefficient of oxygen, γ_O. As a result, despite what is otherwise expected from Eq. 9 (x_{Al} is increased, $\gamma Al = 0.021$ by linear interpolation of binary Cu–Al data in [22]) the molar fraction of O atoms in the melt in equilibrium with alumina might not decrease significantly or might even increase, when the initial aluminum content in the melt is increased. Given the lack of adequate literature data for the Cu8Al–Al_2O_3 system, we cannot repeat estimations presented for the pure Cu–Al_2O_3 system. Still, two mechanisms by which the presence of aluminum in the melt would increase the rate of coarsening of alumina can be suggested. The first comes from the fact that the concentrations of both aluminum and oxygen in the melt might vary with increasing initial aluminum concentration in a way that will increase solute fluxes diffusing through the melt, and hence the rate of alumina transport. The effect can be quantified by Wagner's first-order interaction parameter ε_O^{Al}, which is by definition the rate of change of $\ln(\gamma_O)$ in liquid copper with increasing x_{Al}; if ε_O^{Al} is strongly negative, an increase in x_{Al} will cause x_O predicted by Eq. (9) to increase as well. A value of $\varepsilon_O^{Al} \approx -100$ would explain the present data.

Taking thus $\varepsilon_O^{Al} = -100$, we calculate x_O at 1,423 and 1,573 K with Eq. (9), supposing that ε_O^{Al} stays roughly constant in this temperature range. Then, we can estimate R_0, the smallest radius of curvature one expects to observe along the metal/ceramic interface after infiltration, using Eq. (2). For the volume diffusion coefficient at 1,573 K, we take the value of 10^{-9} m^2/s, deduced from the estimations for the Cu–Al_2O_3 system. The diffusion coefficient at 1,423 K is extrapolated from that at 1,573 K assuming $Q \approx 40$ kJ/mol, this being the activation energy for self-diffusion in liquid copper [26]. Results of the calculations are given in Table 2. One finds that $\varepsilon_O^{Al} \approx -100$ coupled with a dominance of diffusion through the liquid would indeed explain why rounding occurs during infiltration with a Cu8Al melt at 1,573 K. At 1,423 K this assumption predicts no measurable rounding, also in agreement with the present (lower-temperature) infiltration data, see Fig. 4. Since a value of $\varepsilon_O^{Al} \approx -100$ is not absurd (for example, $\varepsilon_O^{Al} = -433$ for aluminum–oxygen interactions in liquid iron [30]), this mechanism offers a first explanation for the present observations.

Table 2 Oxygen concentration and particle rounding parameters predicted for the Wagner interaction parameter $\varepsilon_O^{Al} = -100$

ε_O^{Al}	−100
γ_O	4×10^{-8}
x_O at 1423 K	1×10^{-6}
x_O at 1573 K	4×10^{-4}
R_0 at 1423 K, $\alpha_V = 3$	85 nm
R_0 at 1423 K, $\alpha_V = 7$	113 nm
R_0 at 1573 K, $\alpha_V = 3$	431 nm
R_0 at 1573 K, $\alpha_V = 7$	572 nm

A second mechanism that might cause the strong enhancement in rounding rate of alumina at 1,300 °C when aluminum is added to the copper melt is suggested by observations of Saiz et al. [10]. These authors showed that, when polycrystalline Al_2O_3 contacts molten pure Al, deep grooves are observed at a temperature of 1,100 °C, unlike what is seen with copper. Saiz et al. [10] suggested interfacial diffusion as the responsible mechanism, with a possible contribution from volume diffusion. In sessile drop experiments, the presence of Al in drops resting on Al_2O_3 was also shown to accelerate significantly the rate of surface diffusion (or in other words the mobility of both Al and O) along solid Al_2O_3 surfaces [31]. Now, in [32] it is shown, based on a monolayer thermodynamic model, that aluminum segregates strongly to the interface between alumina and dilute solutions of aluminum in liquid copper (Eq. 26 and Table V of that reference). If the interface between alumina and liquid Cu–Al is strongly enriched in aluminum, it is then to be expected that the mobility of atoms take a character closer to interfacial diffusion along liquid aluminum rather than liquid copper. This, in turn, is known from the work of Saiz et al. [10] to be far more rapid than diffusion along the copper/alumina interface. Working the numbers ($\gamma = 0.7$ J/m^2 and $D_l\omega = 1 \times 10^{-19}$ m^3/s at 1,373 K [10]) in Eq. (3) gives $R_0 = 655$ nm at $T = 1{,}423$ K or 1.410 μm at $T = 1{,}573$ K, for $\Delta t = 180$ s; these values for pure Al are far higher than values observed here with Cu8Al. Aluminum enrichment of the melt/ceramic interface as a result of aluminum addition to the copper melt can thus also account for a significant acceleration of interfacial diffusion.

The strong difference shown by data in the extent of Al_2O_3 rounding in Cu8Al at 1,150 and at 1,300 °C is

indicative of a transport mechanism characterized by a high activation energy: data and Eqs. (2) or (3) suggest $Q \approx 400$ kJ/mol. This is the range of Q values characteristic of one-third of $\Delta G^F_{Al_2O_3}$ but also of the activation energy for surface diffusion along alumina (250–550 kJ/mol [28]). This second mechanism is thus as plausible as is the first with respect to the temperature-dependence of alumina particle rounding in Cu8Al.

Conclusions

The presence of aluminum in copper increases the mobility of the interface between alumina and the molten metal, the effect being strongly temperature-dependent. This, in turn, causes marked capillarity-driven rounding of 5 μm alumina particles after infiltration with Cu8wt%Al at or above 1,300 °C, and is also likely to influence other processes such as brazing. We propose that the phenomenon may result from coupled variations in the concentration of Al and O in the copper melt with the initial metal aluminum content, or from an enhancement of interfacial diffusion caused by a high level of aluminum interfacial segregation along alumina in copper.

Acknowledgements We gratefully acknowledge help from Prof. N. Eustathopoulos of INP Grenoble, with whom we have had several enlightening discussions on the topic of this study. This study was funded by the KTI/CTI Förderagentur für Innovation through CTI project 9026.1 PFIW-IW in collaboration with the company Swissmetal (Dornach, Switzerland).

References

1. Chatain D, Rivollet I, Eustathopoulos N (1986) J Chim Phys Phys Chim Biol 83(9):561
2. Naidich J (1981) Prog Surf Membr Sci 14:353
3. Eustathopoulos N, Drevet B (1994) J Phys III 4(10):1865
4. Eustathopoulos N, Nicholas M, Drevet B (1999) Wettability at high temperatures, Pergamon material series, vol 3. Pergamon, Amsterdam
5. Saiz E, Cannon RM, Tomsia AP (2008) Annu Rev Mater Res 38:197
6. Biselli C, Morris DG, Randall N (1994) Scr Mater 30(10):1327
7. Travitzky NA, Shlayen A (1998) Mater Sci Eng A 244(2):154
8. Nachum S, Fleck NA, Ashby MF, Colella A, Matteazzi P (2010) Mater Sci Eng A 527(20):5065
9. Winzer J, Weiler L, Pouquet J, Roedel J (2011) Wear 271(11–12): 2845
10. Saiz E, Cannon RM, Tomsia AP (1998) Acta Mater 47(15):4209
11. Saiz E, Tomsia AP, Cannon RM (2001) Scr Mater 44(1):159
12. Mortensen A (2000) In: Clyne TW (ed) Comprehensive composite materials, vol 3: Metal matrix composites. (Series editors: Kelly A, Zweben C). Pergamon, Oxford
13. Bahraini M, Molina JM, Kida M, Weber L, Narciso J, Mortensen A (2005) Curr Opin Solid State Mater Sci 9(4–5):196
14. Rasband WS (1997–2011) U.S. National Institutes of Health, Bethesda. http://imagej.nih.gov/ij/
15. Documentation for Vision Assistant (2011) software, National Instruments, Austin, TX, USA
16. Bahraini M, Weber L, Narciso J, Mortensen A (2005) J Mater Sci 40(9–10):2487. doi:10.1007/s10853-005-1980-1
17. Trumble KP (1992) Acta Metall 40:S105
18. Miserez A, Stucklin S, Rossoll A, Marchi CS, Mortensen A (2002) Mater Sci Technol 18(12):1461
19. Doremus RH (2006) J Appl Phys 100(10): 101301-1–101301-17
20. Nichols FA, Mullins WW (1965) Trans Metall Soc AIME 233(10): 1840
21. Kubaschewski O, Alcock CB, Spencer PJ (1993) Materials thermochemistry. Pergamon Press, Oxford
22. Hultgren R (1990) Selected values of the thermodynamic properties of binary alloys. American Society for Metals, Metals Park
23. Kanibolotsky DS, Bieloborodova OA, Kotova NV, Lisnyak VV (2002) J Therm Anal Calorim 70(3):975
24. Schmid R (1983) Metall Trans B 14(3):473
25. Poirier D, Geiger G (1994) Transport phenomena in materials processing. TMS The Minerals, Metals and Materials Society, Warrendale
26. Gale W, Totemeier T (eds) (2004) Smithells metals reference book, 8th edn. Elsevier Butterworth-Heinemann, Amsterdam
27. Iida T, Guthrie R (1988) The physical properties of liquid metals. Clarendon Press, Oxford
28. Tsoga A, Nikolopoulos P (1994) J Am Ceram Soc 77(4):954
29. Jacob KT, Alcock CB (1972) Acta Metall 20(2):221
30. Kubaschewski O, Alcock CB (1979) Metallurgical thermochemistry. Pergamon Press, Oxford
31. Saiz E, Tomsia AP, Suganuma K (2003) J Eur Ceram Soc 23(15): 2787
32. Li JG, Coudurier L, Eustathopoulos N (1989) J Mater Sci 24(3): 1109. doi:10.1007/BF01148806